

FIXED-WING AIRCRAFT PORT-HAMILTONIAN DYNAMICS AND CONTROL

Joao Erick de Mattos Fernandes[1], Flávio Luiz Cardoso Ribeiro[2] & Mauricio Andrés Varela Morales[2]

[1]DSc Student, Aeronautical Engineering, Instituto Tecnológico de Aeronáutica, Brazil
[2]Assistant Professor, Aeronautical Engineering, Instituto Tecnológico de Aeronáutica, Brazil

Abstract

This paper presents an approach to modeling and controlling fixed-wing aircraft longitudinal dynamics utilizing the port-Hamiltonian (pH) framework. In this work, the complete aircraft longitudinal model is derived by interconnecting inertial, rotational, and quasi-stationary aerodynamic subsystems. To achieve precise trajectory tracking during approach phases, a pH control law based on generalized canonical transformations is implemented, which explicitly accommodates time-dependent tracked variables. The proposed model and controller are validated in a simulated decelerating, descent and leveling-off scenario representative of an Instrument Landing System (ILS) approach. Results are compared against a benchmark TECS controller as both methods successfully manage the flight profile.

Keywords: Port-Hamiltonian dynamics, Flight dynamics, Port-Hamiltonian control, Canonical transformation of port-Hamiltonian systems

1. INTRODUCTION

Understanding and controlling airplanes based on assessing and modifying their energy states is not an unusual concept. Pilot training to this date focuses on this task, as can be seen in the “Airplane Flying Handbook” [1] published by FAA. This publication dedicates a full chapter on energy management, and concepts such as kinetic and potential energy and their relationship with airplane commands in different flight situations.

The development of a flight control technique known as TECS (Total Energy Control System) follows the same logic by controlling the total energy of the airplane and the energy distribution [2, 3, 4]. However, TECS was conceived from a Newtonian representation of the longitudinal dynamics of airplanes. A representation based on energy would be more suitable both for visualization and implementation of such system.

Port-Hamiltonian systems, as introduced by [5, 6] enables modeling, simulation and control of physical systems and the interconnection of them. Several engineering applications approach were conducted such as [7, 8], that proposed a framework for modeling and control of water channels. Other works include [9] that studied a fluid-structure interaction prototype that mimics a flexible airplane wing with piezoelectric actuators and tip-tank, and applied a passivity-based control technique for damping injection. Also, [10] used the same approach for modeling and control of complex structural dynamics of civil engineering structures, such as a high-rise building.

Several works can also be found on the aerospace field. For instance, [11] and [12] proposed a model and control of quadcopters. Even more aligned with the present work, for the fixed-wing dominium, some very meaningful advancement was made by [13] and their more recent works [14, 15]. They were able to introduce some terms of the aerodynamics - which poses a challenge since aerodynamic forces both introduces and removes energy from the system - and obtain a port-Hamiltonian description of the airplane dynamics. This approach made possible the derivation of a control based

on [16]. These later works, however, used some simplifications that hindered the simulation of the dynamics using the model whose control was based.
Recently, these authors proposed a fixed-wing longitudinal model that, for the first time, enabled a simulation solely with the use of a port-Hamiltonian system in [17]. While previous efforts to incorporate complex aerodynamic forces into port-Hamiltonian descriptions were limited by simplifications that prevented direct simulation, recent advancements [17] have introduced a longitudinal model that allows for the first complete simulation of fixed-wing dynamics using a port-Hamiltonian framework.

1.1 Classical Approach vs port-Hamiltonian framework

The port-Hamiltonian framework offers several distinct advantages over classical models, most notably its inherent modularity and energy accountability [18]. While other modeling paradigms allow for system interconnections, the pH framework is constructed around this philosophy, enabling the interaction of several different types of physical systems.
The basic outline of a port-Hamiltonian system is

$$\begin{matrix} \dot{x} = (J-R)\nabla_x H + gu \\ y = g^T \nabla_x H \end{matrix} \quad ; \quad \text{being} \quad H = \frac{1}{2} p^T M^{-1} p + U \tag{1}$$

where U comprises the sum of all system potential energy.

1.2 Work outline

This work is organized as follows: Section 2. comprises a reconstruction of the longitudinal fixed-wing airplane model from inertial, rotational and aerodynamic subsystems. Section 3. covers port-Hamiltonian control and its challenges, placing an emphasis on Canonical Transformation. Lastly, a simulation is carried in order to compare the port-Hamiltonian model and control with classical approaches on Section 4..

2. FIXED-WING AIRCRAFT PORT-HAMILTONIAN LONGITUDINAL MODEL

The classical longitudinal model for fixed-wing airplanes can be derived directly from the forces acting on the vehicle with varying degrees of complexity.
For this work, the forces considered are depicted in the figure below. Scalar equations can easily be derived from the previous model, rendering the following set of equations.

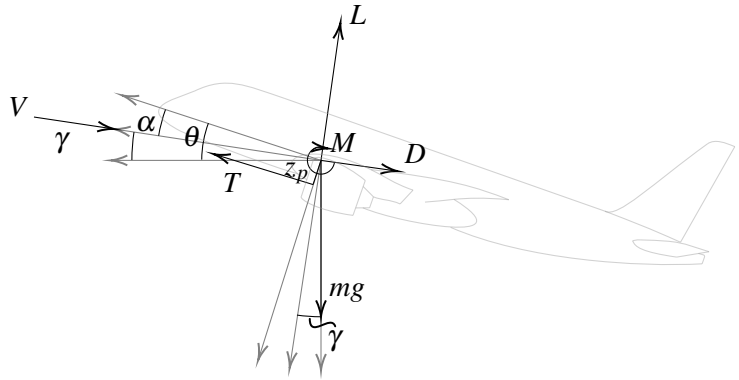


Figure 1 – Classical Model Variables.

$$\begin{aligned} \dot{V} &= \frac{1}{m}\left(-D + T\cos(\alpha) - mg\sin(\gamma)\right) \\ \dot{\alpha} &= q + \frac{1}{mV}\left(-L - T\sin(\alpha) + mg\cos(\gamma)\right) \\ \dot{q} &= \frac{1}{I_{yy}}\left(M + z_p T\right) \\ \dot{\theta} &= q \\ \dot{h} &= V\sin(\gamma) \\ \dot{x} &= V\cos(\gamma) \end{aligned} \tag{2}$$

The previous equations are largely applied to modeling and simulation [19]; therefore, they are used in the development of control laws applied in the aviation industry. It constitutes a solid benchmark against which a properly developed model can be compared.
The first aim of this work is to derive energy-based equations matching 2, which will be carried out in the following sections.

2.1 Inertial System

The inertial system reduces the airplane to a point-mass system and deals solely with gravitational potential and kinetic energy.

There is no dissipation since the Drag force D is embedded in F_H, which is a system input parallel to V .The input forces considered are applied vertically and horizontally in reference to the mass displacement, not to the inertial reference frame. For the same reason, T is not considered. Additionally, T effects depend on α, which is not a variable for the system at this point. Thrust, nevertheless, can be added by summing its effects to inputs L and D.

The main operator in this system is γ, which defines the rate of change between kinetic and potential energy. This system has $x = [q \quad p]^\top = [x \quad h \quad mV_x \quad mV_h]^\top$ and Hamiltonian $H = \frac{p_{V_x}^2 + p_{V_h}^2}{2m} + mgh$:

$$\dot{x} = \begin{pmatrix} \dot{x} \\ \dot{h} \\ m\dot{V}_x \\ m\dot{V}_h \end{pmatrix}; \quad J = \begin{pmatrix} 0 & 0 & 1 & 0 \\ 0 & 0 & 0 & 1 \\ -1 & 0 & 0 & 0 \\ 0 & -1 & 0 & 0 \end{pmatrix}; \quad B = \begin{pmatrix} 0 & 0 \\ 0 & 0 \\ \frac{V_h}{(V_x^2+V_h^2)^{1/2}} & \frac{V_x}{(V_x^2+V_h^2)^{1/2}} \\ \frac{V_x}{(V_x^2+V_h^2)^{1/2}} & \frac{-V_h}{(V_x^2+V_h^2)^{1/2}} \end{pmatrix}; \quad u = \begin{pmatrix} F_V \\ -F_H \end{pmatrix} \tag{3}$$

Alternatively, using the pair V and γ, which are more familiar for this kind of system, as can be inferred by Equation 2, the same system can be rewritten in the following form:

$$\dot{x} = \begin{pmatrix} \dot{x} \\ \dot{h} \\ m\dot{V} \\ mV\dot{\gamma} \end{pmatrix}; \quad J = \begin{pmatrix} 0 & 0 & \cos(\gamma) & 0 \\ 0 & 0 & \sin(\gamma) & \cos(\gamma) \\ -\cos(\gamma) & -\sin(\gamma) & 0 & 0 \\ 0 & -\cos(\gamma) & 0 & 0 \end{pmatrix}; \quad B = \begin{pmatrix} 0 & 0 \\ 0 & 0 \\ 0 & 1 \\ 1 & 0 \end{pmatrix} \tag{4}$$

Input vector remains unchanged and Hamiltonian is given by $H = \frac{p_V^2}{2m} + mgh$.

It is also important to highlight that γ varies only with $\dot{\gamma}$, which, in turn, is controlled by L. This dynamic does not affect $\dot{H}$, given that L is a centripetal force. For this reason, $y = [0 \quad V]^T$. This system is representative of the phugoid mode of the airplane, where a disturbance would cause a lightly dampened harmonic tradeoff of potential and kinetic energy, as long as the interdependence of F_V and F_H is respected.

2.2 Rotational Dynamics

The rotational dynamics account for the aircraft's motion about its center of mass, decoupled from the rotational components induced by changes in the flight path angle, $\dot{\gamma}$.

The angular acceleration, defined as $\dot{A} = \ddot{\alpha}$, is governed by three primary torque components: the commanded torque τ_c applied by the elevator; a dissipative aerodynamic damping torque $M_q A$; and a restorative 'spring' torque $G_\alpha \alpha$. The latter is proportional to the angle of attack α and represents the potential energy contribution to the system's Hamiltonian.

$$\dot{x} = \begin{pmatrix} \dot{\alpha} \\ I_{yy}\dot{A} \end{pmatrix}; \quad J = \begin{pmatrix} 0 & 1 \\ -1 & 0 \end{pmatrix}; \quad R = \begin{pmatrix} 0 & 0 \\ 0 & -M_q \end{pmatrix}; \quad B = \begin{pmatrix} 0 \\ 1 \end{pmatrix}; \quad u = \tau_c \tag{5}$$

The Hamiltonian is, therefore, given by:

$$H = \frac{p_\alpha^2}{2I_{yy}} + \frac{G_\alpha \alpha^2}{2} \tag{6}$$

In this formulation $y = \dot{\alpha}$.

This system is representative of the short period mode of the airplane, where an excitation of α would initiate an oscillatory motion around the center of gravity, dampened by M_q.

2.3 Aerodynamic System

For the Aerodynamic System, the primary concern is to build a model that supplies the quasi-stationary values for the stationary behavior, using an input vector of $u = [V \quad V\alpha \quad \dot{\alpha}]^\top$:

$$\begin{aligned} C_L &= C_{L_0} + C_{L_\alpha}\alpha + C_{L_q}(\frac{\dot{\alpha}c}{2V}) \\ C_D &= C_{D_0} + C_{D_\alpha}\alpha + C_{D_{\alpha^2}}\alpha^2 + C_{D_q}(\frac{\dot{\alpha}c}{2V}) \\ C_m &= C_{m_0} + C_{m_\alpha}\alpha + C_{m_q}(\frac{\dot{\alpha}c}{2V}) \end{aligned} \tag{7}$$

This formulation differs from the classical approach in not providing the stability derivatives and their dependencies regarding control. This is deliberate since the control inputs for the interconnected system are forces and moments exerted in the boundary of the system.
Assuming there are velocities for the air around the airfoil that could be different from the airplane velocity vector $V_f = [u_f \quad w_f \quad q_f]^\top$, the output for the port-Hamiltonian Aerodynamic system is thus:

$$\mathbf{y} = \begin{pmatrix} D \\ L \\ M \end{pmatrix} = \frac{qS}{V} \begin{pmatrix} C_{D_0} & (C_{D_\alpha} + C_{D_{\alpha^2}}\alpha) & \frac{cC_{D_q}}{2} \\ C_{L_0} & C_{L_\alpha} & \frac{cC_{L_q}}{2} \\ cC_{m_0} & cC_{m_\alpha} & \frac{c^2C_{m_q}}{2} \end{pmatrix} \begin{pmatrix} u_f \\ w_f \\ q_f \end{pmatrix} \tag{8}$$

In case the air velocity vector matches its counterpart for the airplane ($[u_f \quad w_f \quad q_f]^\top = [(V\cos(\alpha) \approx V) \quad (V\sin(\alpha) \approx V\alpha) \quad \dot{\alpha}]^\top$), the aerodynamic forces are given by the aerodynamic system of 7, when the derivatives are multiplied by qS for forces or qSc for moments.
Following the surrounding airspeed assumption, the Hamiltonian is then:

$$H = \frac{p_z^2}{2m_z} + \frac{p_x^2}{2m_x} + \frac{p_\theta^2}{2I} \tag{9}$$

Where $m_z = \rho\pi\left(\frac{c}{2}\right)^2 b$, $m_x = \rho\pi\left(\frac{t}{2}\right)^2 b$, and $I = \frac{\rho\pi b}{8}\left(\frac{c}{2}\right)^4$.
The remainder matrices are not relevant to this present work, since the port-Hamiltonian model presented here will not deal with aerodynamic transients. Additionally, the apparent masses described by m_x and m_z are mostly negligible when dealing with airplane dynamics. Bottom line, for the purpose of the present work, only the quasi-stationary part of the model will be considered.

2.4 Interconnections

Before interconnecting the system, the next figure non-exhaustively shows how the main interactions among the systems produce a trajectory and airspeed change through the input of a control moment and thrust.

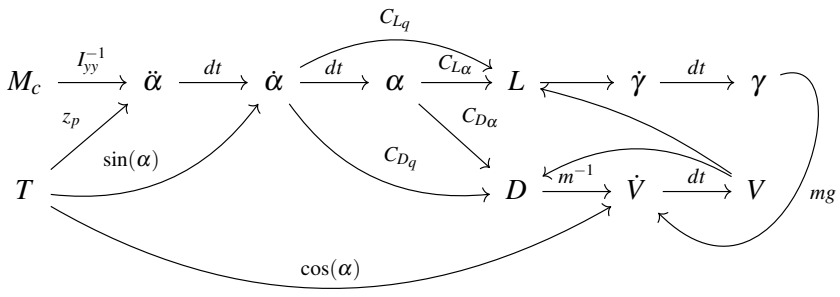


Figure 2 – Model main interactions

It is imperative to note that the input must be a moment applied in the boundary of the system, as stated before, and its magnitude is relative to the control input generated torque only. Nevertheless, the effect of this moment must be dealt with by the entire aerodynamic behavior of the aircraft. For that reason, although Lift and Drag are presented as a closed value for their effects - both divided by V to produce L_V and D_V - parts of the aerodynamic system governing moments must appear in the final port-Hamiltonian form.
Interconnecting the above subsystems, therefore, renders the final form of the port-Hamiltonian model as expressed by the equations below, considering $[\dot{q} \quad \dot{p}]^\top = \begin{bmatrix} \dot{x} & \dot{h} & \dot{\alpha} & m\dot{V} & mV\dot{\gamma} & I_{yy}\dot{A} \end{bmatrix}^\top$.

$$J = \begin{pmatrix} 0 & 0 & 0 & \cos(\gamma) & 0 & 0 \\ 0 & 0 & 0 & \sin(\gamma) & \cos(\gamma) & 0 \\ 0 & 0 & 0 & 0 & 0 & 1 \\ -\cos(\gamma) & -\sin(\gamma) & 0 & 0 & -L_V & 0 \\ 0 & -\cos(\gamma) & 0 & L_V & 0 & 0 \\ 0 & 0 & -1 & 0 & 0 & 0 \end{pmatrix}; \qquad B = \begin{pmatrix} 0 & 0 & 0 \\ 0 & 0 & 0 \\ 0 & 0 & 0 \\ -D_{M_c} & 0 & \cos(\alpha) \\ L_{M_c} & 0 & \sin(\alpha) \\ 1 & 1 & z_p \end{pmatrix} \tag{10}$$

For this final system, $R = \text{diag}([0 \quad 0 \quad 0 \quad D_V \quad 0 \quad -M_q])$ and $u = [\tau_c \quad \tau_0 \quad T]^T$, where τ_c is the commanded elevator moment, τ_0 is the trim torque and T the engine thrust.
Since there is no superposition of dynamic behavior, the final Hamiltonian should be the sum of the individual subsystem Hamiltonians:

$$H = \frac{1}{2} p^\top M^{-1} p + V(q) = \frac{p_V^2}{2m} + \frac{p_{\dot{\alpha}}^2}{2I_{yy}} + \frac{G_\alpha \alpha^2}{2} + mgh \tag{11}$$

It is important to note that no Hamiltonian elements for the Aerodynamic System are present since this system deals with the fluid and not the airplane. The aerodynamic effects are accounted for when Lift and Drag forces, in terms of the Aerodynamic system, are considered.

3. PORT-HAMILTONIAN CONTROL

Control of the port-Hamiltonian system is achieved by either an interconnection with a secondary port-Hamiltonian system or a transformation of the original system. In any case, control laws must result in a final system that obeys the port-Hamiltonian structure. This prerequisite narrows the options for control compared with the myriad of options for linear systems and constitutes a research field on its own, according to [6].
Some of the approaches are Damping Injection, Energy Shaping and Passivity-based control, as briefly discussed below:

3.1 Damping Injection

One common approach is the use of dissipative control, which basically increases the stability or rate of dissipation of the system by use of a control law such as $u = -Cy$. This is typically achieved by adding a feedback term to the system dynamics that drives the energy towards a desired state of minimum energy. For instance, in the case of mechanical systems, a common form of port-Hamiltonian control law might involve a feedback that is proportional to the velocity (momentum), ensuring that energy is dissipated as the system moves toward equilibrium point.

3.2 Energy shaping

Energy shaping in a control technique based on the interconnection of systems, where a secondary control system is connected to the port-Hamiltonian original plant. The total energy $H_t = H + H_c$ is then used as a Lyapunov function candidate. An equilibrium point other than the minimum energy state can be chosen with the aid of a Casimir function. The challenge to this control technique is to find such control system, since the Casimir function dictates a set of restrictions, being the most important a "dissipation obstacle" [6], which prevents the use of this technique in most mechanical applications.

3.3 Interconnection and Damping Assignment-Passivity-Based Control

IDA-PBC, as it is commonly referred to, is a technique that expands the possibilities of system interconnection. Not only the Hamiltonian function is a design parameter but also the framework matrices J_d and R_d, being the d subscript for "desired". Nonetheless, these parameters are not independent, which rises two possibilities for the method implementation:

- Non-parametrized IDA-PBC - where J_d and R_d are set and the controller is given by the resolution of the PDE $\partial H_d/\partial x$. The solution satisfying $x^* \arg\min\{H_d\}$ is selected.
- Algebraic IDA-PBC - where H_d is fixed, producing an algebraic set of equations depending on J_d and R_d.
- Parametrized IDA-PBC - where H_d is fixed, imposing constraints in J_d and R_d.

3.4 Trajectory Tracking via generalized canonical transformations

Trajectory tracking via generalized canonical transformations is a technique that further expands the limits of IDA-PBC by enabling the control of a time-varying Hamiltonian function [16]. This technique preserves passivity even with a time varying desired Hamiltonian function. A time varying desired signal is therefore possible.
According to [16], for purely mechanical systems, a passive error system with a positive definite Hamiltonian regarding track error can be obtained from the Equations 12.

$$\begin{aligned} \bar{H} &= H(q,p) + \frac{1}{2}\dot{q}^d(t)^\top M(q)\dot{q}^d(t) - p^\top \dot{q}^d(t) + \bar{U}(q-q^d)(t)) \\ \bar{q} &= q - q_d(t) \\ \bar{y} &= M(q)^{-1}p - \dot{q}_d(t) \\ \bar{u} &= u - M\ddot{q}_d(t) + \frac{\partial \bar{U}^\top}{\partial q} + \left(\frac{1}{2}\frac{\partial (M(q)\dot{q}_d)^\top}{\partial q} - \frac{1}{2}\frac{\partial (M(q)\dot{q}_d)}{\partial q} + \frac{1}{2}M\frac{\partial (M^{-1}(q)p)}{\partial q} - D\right)\dot{q}_d(t) \end{aligned} \tag{12}$$

In this formulation, $\bar{U}$ is a free design parameter representing the virtual potential energy and, therefore, should be positive definite. The matrix D is a positive semi-definite matrix containing the dissipation elements associated with $\frac{\partial H(q,p)^\top}{\partial p}$, representing the viscous dissipation. For the system studied in this work, $D = diag(D_V, D_V, M_q)$, since these are the dissipation associated with $\dot{x}$, $\dot{h}$ and $\dot{\alpha}$.
For the longitudinal airplane system, a valid canonical transformation aided by equations 12 can be achieved by the following values:

$$\bar{U} = \frac{1}{2}\left(K_x(x-x_d)^2 + (K_h(h-h_d)^2 + (K_\alpha(\alpha-\alpha_d)^2\right) + mgh \tag{13}$$

$$\bar{q} = \begin{bmatrix} x - x_d \\ h - h_d \\ \alpha - \alpha_d \end{bmatrix} = \begin{bmatrix} x - \frac{\dot{V}_d}{2}\cos(\gamma_d)t^2 + V_0 t\cos(\gamma_d) + x_0 \\ h - \frac{\dot{V}_d}{2}\sin(\gamma_d)t^2 + V_0 t\sin(\gamma_d) + h_0 \\ \alpha - \alpha_d \end{bmatrix} \tag{14}$$

$$\dot{\bar{q}} = \begin{bmatrix} \dot{x} - \dot{x}_d \\ \dot{h} - \dot{h}_d \\ \dot{\alpha} - \dot{\alpha}_d \end{bmatrix} = \begin{bmatrix} \dot{x} - V_{x_0} + \dot{V}_d\cos(\gamma_d)t \\ \dot{h} - V_{y_0} + \dot{V}_d\sin(\gamma_d)t \\ \dot{\alpha} - 0 \end{bmatrix} \tag{15}$$

$$\ddot{\bar{q}} = \begin{bmatrix} \ddot{x} - \ddot{x}_d \\ \ddot{h} - \ddot{h}_d \\ \ddot{\alpha} - \ddot{\alpha}_d \end{bmatrix} = \begin{bmatrix} \ddot{x} - \dot{V}_d\cos(\gamma_d) \\ \ddot{h} - \dot{V}_d\sin(\gamma_d) \\ 0 \end{bmatrix} \tag{16}$$

These parameters, along with Equation 17, render the effort needed to stabilize the system in the desired trajectory.

$$u_{prel} = M\ddot{q}^{\mathsf{d}}(t) - \frac{\partial \bar{U}^{\mathsf{T}}}{\partial q} - \frac{1}{2}\frac{\partial (M(q)\dot{q}^{\mathsf{d}})^{\mathsf{T}}}{\partial q}\dot{q}^{\mathsf{d}}(t) + \frac{1}{2}\frac{\partial (M(q)\dot{q}^{\mathsf{d}})}{\partial q}\dot{q}^{\mathsf{d}}(t) - \frac{1}{2}M\frac{\partial (M^{-1}(q)p)}{\partial q}\dot{q}^{\mathsf{d}}(t) + D\dot{q}^{\mathsf{d}}(t) - C\bar{y} \tag{17}$$

After the calculation of Equation 17, considering the values of Equations 14, 15 and 16, a final control law for a totally actuated system is presented in Equation 18. Additionally, since the control inputs for the system are, according to the system presented by Equation 10, τ_c and T, a transformation has to be carried on, considering the geometric aspects of the system as described by Figure 1.

$$u_{prel} = \begin{bmatrix} F_x \\ F_h \\ \tau_{c_{req}} \end{bmatrix} = \begin{bmatrix} m\ddot{x}_d - C_1(V_x - \dot{x}_d) - 2k_x(x - x_d) + D_V\dot{x}_d \\ m\ddot{h}_d - C_2(V_h - \dot{h}_d) - 2k_h(h - h_d) + D_V\dot{h}_d + mg \\ -k_\alpha(\alpha - \alpha_d) - C_3\dot{\alpha} \end{bmatrix} = \begin{bmatrix} \cos(\alpha+\gamma) & -\sin(\gamma) \\ \sin(\alpha+\gamma) & \cos(\gamma) \\ 0 & 1 \end{bmatrix} \begin{bmatrix} T_{req} \\ L_{req} \\ \tau_{c_{req}} \end{bmatrix} \tag{18}$$

In order to produce the desired lift amount and match the real actuation of the system, the necessary lift L_{req} shall be embedded in $\tau_{c_{req}}$ in a manner that the change in α supplies the Lift the system needs. This is accomplished by the relations depicted by Equation 19, where $L_{0_{req}}$ accounts for all the lift that is generated that does not relate to α. Not accounting for $L_{0_{req}}$ would produce a α_d greater than the one needed for producing L_{req}.

$$\alpha_d = \frac{2(L_{req} - L_{0_{req}})}{C_{L_\alpha}\rho V_d^2 S} \quad \text{where} \quad L_{req} = F_h\cos(\alpha+\gamma)\sec(\alpha) - F_x\sin(\alpha+\gamma)\sec(\alpha) \quad \text{and} \quad L_{0_{req}} = \frac{C_{L_{0_d}}\rho V_d^2 S}{2}; \tag{19}$$

Final control law is shown in Equation 20. A direct relation of T_{req} and $\tau_{c_{req}}$ to $\dot{V}_d$ and γ_d - the actual variables being controlled - can be derived recursively with Equations 14, 15, 16, 18 and 19. This final form is omitted for brevity, as it does not further elucidate the core methodology of this work.

$$\begin{aligned} T_{req} &= F_x\cos(\gamma)\sec(\alpha) + F_h\sin(\gamma)\sec(\alpha) \\ \tau_{c_{req}} &= -k_\alpha(\alpha - \alpha_d) - C_3\dot{\alpha} \end{aligned} \tag{20}$$

The above control law, along with the derived Hamiltonian system, are used in the simulations. The control parameters $\dot{V}_d$ and γ_d are ideal to enable the comparison to the benchmark control method presented in the next section.

4. SIMULATION AND COMPARISON TO CLASSICAL APPROACH

For a fair comparison to the method presented in this work, the Total Energy Control System was selected as the Classical approach method both for its non-linearity and for the validated energy-based approach.

4.1 Total Energy Control System - TECS

The Total Energy Control System (TECS) is an integrated control architecture that manages a fixed-wing aircraft's longitudinal dynamics by treating engine thrust and elevator deflection as tools for energy flow and allocation. Introduced by Lambregts [20], this method calculates the aircraft's total energy state (E) as the sum of its potential energy (mgh) and kinetic energy ($\frac{1}{2}mV^2$). The core logic of TECS is that engine thrust (T) is the primary control for managing the total energy rate ($\dot{E}$), while the flight path - through elevator input - is utilized to rate of transformation between altitude and airspeed.

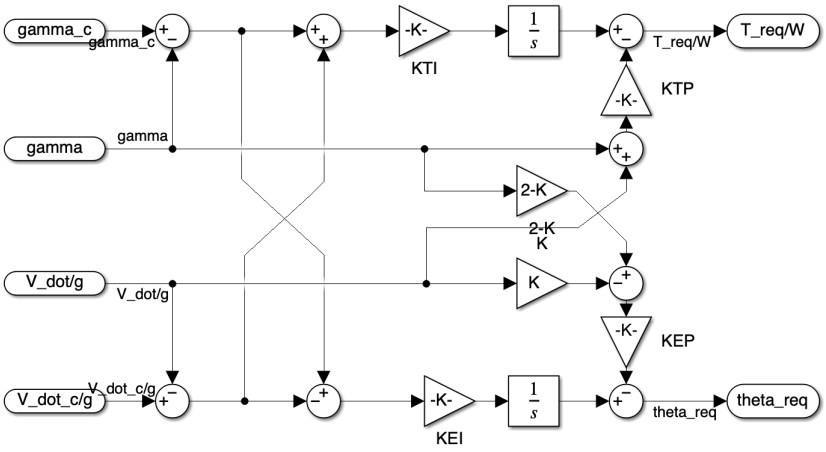


Figure 3 – Total Energy Control System

This approach replaces independent SISO (Single-Input Single-Output) loops with a coordinated system that views flight path and speed through the lens of physics-based energy trades.
Implementation of the TECS regulator involves generating demand signals for thrust (δT_c) and pitch ($\delta \theta_c$) based on energy error rates. To ensure the system operates without undesirable coupling, the regulator gains must be constrained such that the total energy rate error and the energy distribution rate error reach zero simultaneously. These demand signals are eventually converted into control inputs through a plant-dependent autopilot, facilitating precise trajectory tracking and airspeed management.

4.2 Simulation scenario

A scenario of a descent profile with multiple levelings off, also including decelerations, was chosen to present the capabilities of both methods, enabling the performance comparison. This procedure is very representative since it is commonly applied to approach procedures.

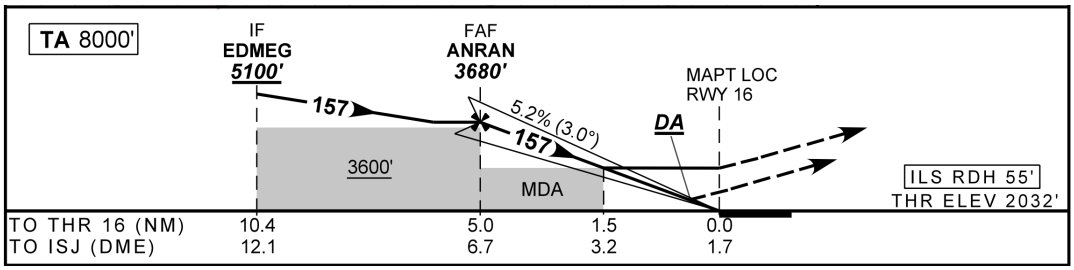


Figure 4 – ILS V RWY16 - Sao Jose dos Campos - Vertical Profile

The controller task is to level off at 5100 feet at 200 knots, 15 nautical miles from the runway threshold—a bit less than five miles prior to the EDMEG position—decelerate to 160 knots until EDMEG, descend in a 3 degree flight path to 3680 feet before reaching the ANRAN position, where it should be leveled off, and then descend to the Decision Altitude of 2232 feet while decelerating to 140 knots. It is important to note that, due to the simplicity of the aerodynamic system used in the simulation, these speeds produce high angles of attack. A more detailed aerodynamic system would take into account the use of flaps and slats, as well as the aerodynamic effects produced by the landing gear. Such refinements would be advantageous to the controller since more drag would be added; therefore, enabling higher possible values for deceleration and glide path.
The controller commands are based on the distance from the runway threshold, as they would be if the autopilot were receiving its orders from a Flight Management and Guidance System.
This profile is very representative of the autopilot tasks during actual operations.

4.3 Simulation Results

The overall simulation result can be seen in the figure 5 where the path is depicted for both controllers and can be compared to the path shown in figure 4:

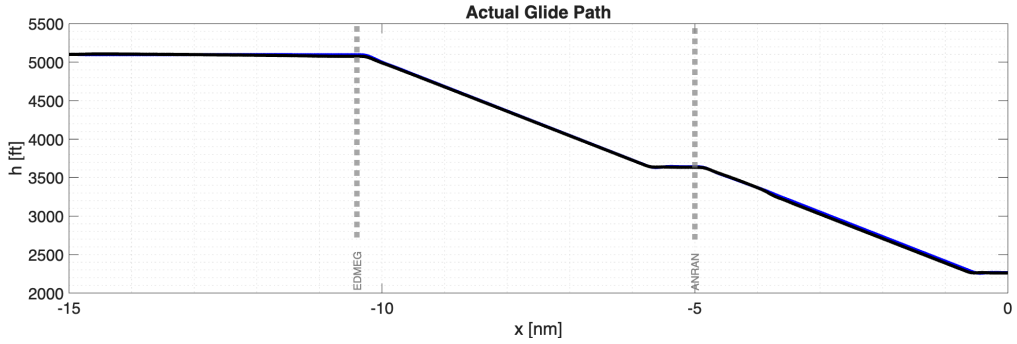


Figure 5 – Simulation Results - Vertical Path

The real qualitative analysis comes, however, from the states, which are depicted in Figure 6.

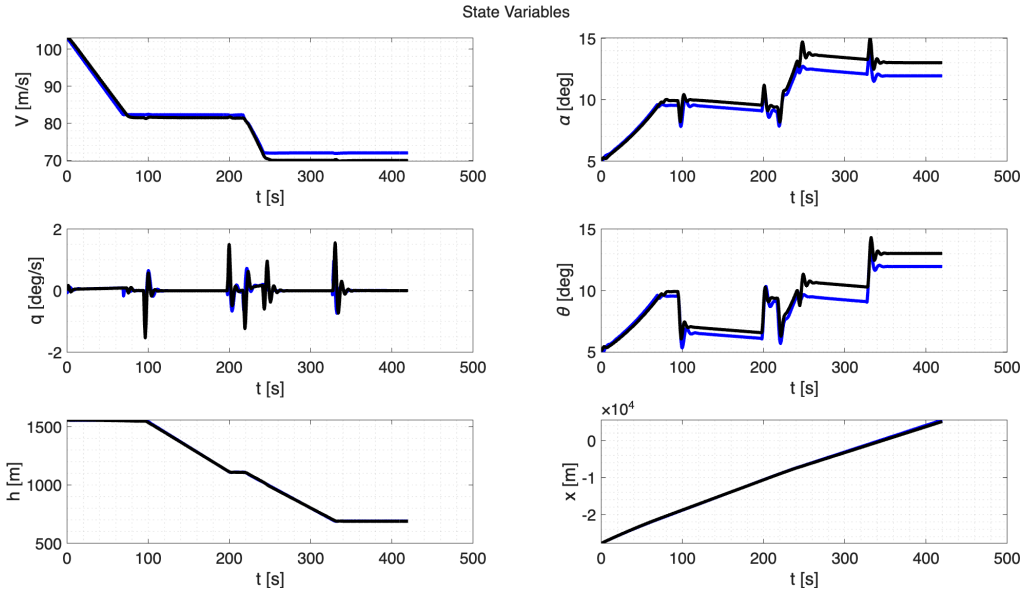


Figure 6 – Simulation Results - State Variables

An analysis of these values reveals that the distinct theoretical approaches employed by each controller yield slight, observable variations in the aircraft states. The root cause for this difference is the management of speed. The subtle difference in airspeed is the source of a more pronounced difference on α that is, as expected, carried out to θ.

State derivatives are also presented to complete the state-space picture of the simulation as can be seen in Figure 7.

In Figure 7 the differences of each control method approach becomes more visible. While TECS provides more subtle control inputs, the hamiltonian control produces more acute variations. Undoubtedly this behavior can be attenuated by a more judicious choice of the control design parameters. Nevertheless, the first seconds of simulation, specially regarding $\dot{V}$ values, demonstrate that due to the difference between approaches, hamiltonian control behavior might not converge to TECS less intense approach.

For the control inputs, the reached values are found in Figure 8.

In these figures, once again the difference in airspeed V produces a slight difference in the magnitude of the control input, specially in regard of elevator deflection angle. A larger α is required for low airspeeds in order to produce the same lift, as depicted by Figure 2.4. This, in turn, translates into higher elevator input.

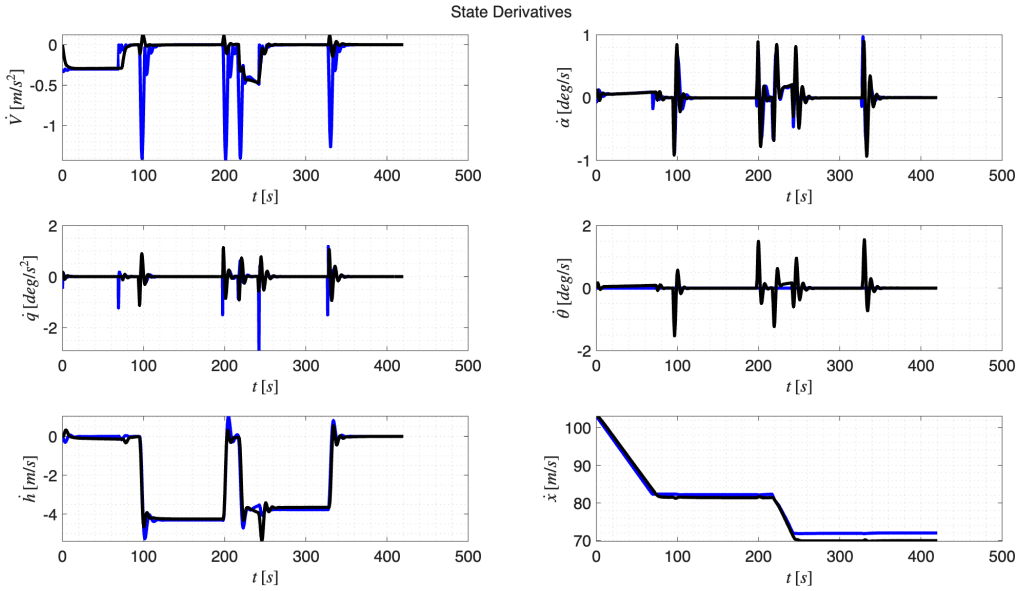


Figure 7 – Simulation Results - State Derivatives

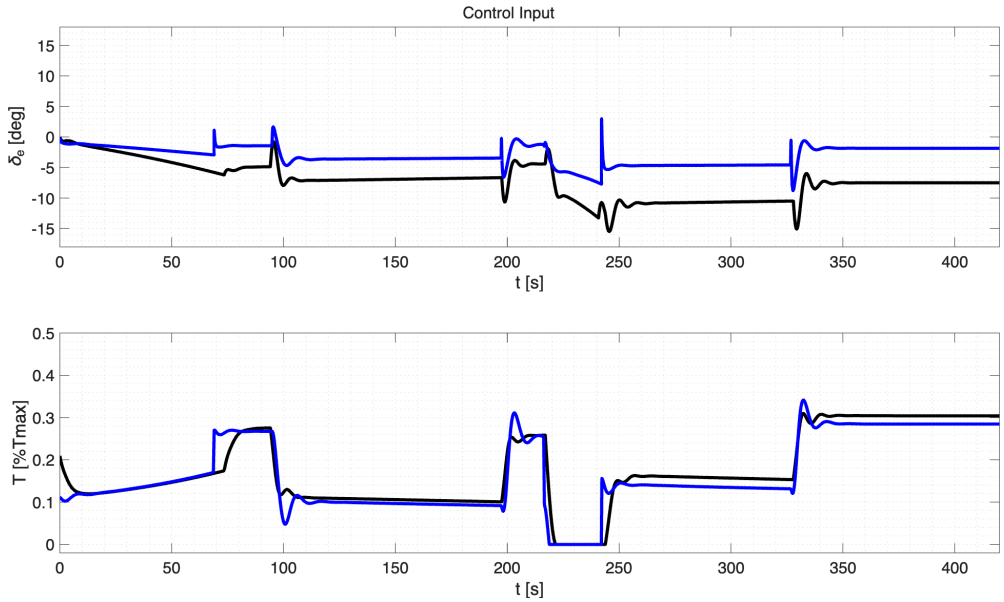


Figure 8 – Simulation Results - Control Inputs

It is also important to point out that in the approximate interval of seconds 220 and 245, both controllers reach a lower boundary saturation, since, for obvious physical reasons $\%T_{max}$ should be kept in the interval between 0 and 1. Nonetheless the controllers kept working as expected despite the saturation.

5. CONCLUSIONS

This work aimed to control the longitudinal flight of a fixed-wing aircraft modeled in the port-Hamiltonian system framework. First, the step-by-step derivation of a canonic port-Hamiltonian system was presented. A control based on the work of [16] was implemented, enabling the comparison against TECS, introduced by [20] and extensively researched, qualifying it as the benchmark.

Both methods successfully accomplished the task of controlling the aircraft through the vertical path of an ILS approach while employing different methodologies. The use of Canonical Transformation as the method of choice for the port-Hamiltonian system control is justified by the explicit dependence on time for the tracked variables.

While TECS is an applied method with straightforward implementation, control via Canonical Trans-

formations, as described by [16], is a generic approach to controlling port-Hamiltonian systems. Its implementation is relatively cumbersome, compared to TECS. However, its value resides in enabling control to complex systems and tracking time dependent variables.
Another contrast that must be pointed out is that while TECS is a system native to a Newtonian framework and takes advantage of an energy approach formulation, control via Canonical Transformation is native to an energy framework and aims to control trajectories, rather than energy itself.
Building upon the feasibility demonstrated in this work, the development of a less generic, purely energy-based control presents a logical next step for future studies.

6. Contact Author Email Address

For further information, please mailto: joao.fernandes@ga.ita.br

7. Copyright Statement

The authors confirm that they, and/or their company or organization, hold copyright on all of the original material included in this paper. The authors also confirm that they have obtained permission, from the copyright holder of any third party material included in this paper, to publish it as part of their paper. The authors confirm that they give permission, or have obtained permission from the copyright holder of this paper, for the publication and distribution of this paper as part of the ICAS proceedings or as individual off-prints from the proceedings.

References

[1] Federal Aviation Administration. *Airplane flying handbook (FAA-H-8083-3A)*. Skyhorse Publishing Inc., 2011.

[2] James R Kelly, Lee H Person, and Kevin R Bruce. Flight testing tecs—the total energy control system. Technical report, SAE Technical Paper, 1986.

[3] Kevin Bruce, JR Kelly, and L Person, JR. Nasa b737 flight test results of the total energy control system. In *Astrodynamics Conference*, page 2143, 1986.

[4] H Spark, PJ González, C Ruwisch, W Meyer-Brügel, and FJ Silvestre. An assessment of aircraft control via siso control loops and total energy control. 2021.

[5] Vincent Duindam, Alessandro Macchelli, Stefano Stramigioli, and Herman Bruyninckx. *Modeling and control of complex physical systems: the port-Hamiltonian approach*. Springer Science & Business Media, 2009.

[6] Arjan Van Der Schaft, Dimitri Jeltsema, et al. Port-hamiltonian systems theory: An introductory overview. *Foundations and Trends® in Systems and Control*, 1(2-3):173–378, 2014.

[7] Boussad Hamroun, Laurent Lefèvre, and Eduardo Mendes. Port-based modelling for open channel irrigation systems. *Transactions on Fluid Mechanics*, 1(12):995–1009, 2006.

[8] Boussad Hamroun, Alexandru Dimofte, Laurent Lefèvre, and Eduardo Mendes. Control by interconnection and energy-shaping methods of port hamiltonian models. application to the shallow water equations. *European Journal of Control*, 16(5):545–563, 2010.

[9] Flávio Luiz Cardoso-Ribeiro, Denis Matignon, and Valérie Pommier-Budinger. A port-hamiltonian model of liquid sloshing in moving containers and application to a fluid-structure system. *Journal of Fluids and Structures*, 69:402–427, 2017.

[10] Alexander Warsewa, Michael Böhm, Oliver Sawodny, and Cristina Tarín. A port-hamiltonian approach to modeling the structural dynamics of complex systems. *Applied Mathematical Modelling*, 89:1528–1546, 2021.

[11] Burak Yüksel, Cristian Secchi, Heinrich H Bülthoff, and Antonio Franchi. Reshaping the physical properties of a quadrotor through ida-pbc and its application to aerial physical interaction. In *2014 IEEE International Conference on Robotics and Automation (ICRA)*, pages 6258–6265. IEEE, 2014.

[12] Yuhu Wu, Kaijian Hu, and Xi-Ming Sun. Modeling and control design for quadrotors: A controlled hamiltonian systems approach. *IEEE Transactions on Vehicular Technology*, 67(12):11365–11376, 2018.

[13] Jean-Michel W. Fahmi and Craig A. Woolsey. Directional stabilization of a fixed-wing aircraft using potential shaping. *2018 Atmospheric Flight Mechanics Conference*, 2018.

[14] Jean-Michel W. Fahmi and Craig A. Woolsey. Cross-track control of rotorcraft using passivity based techniques. *AIAA Scitech 2021 Forum*, 2021.

[15] Jean-Michel Fahmi and Craig A. Woolsey. Port-hamiltonian flight control of a fixed-wing aircraft. *IEEE Transactions on Control Systems Technology*, 30(1):408–415, 2022.

[16] Kenji Fujimoto, Kazunori Sakurama, and Toshiharu Sugie. Trajectory tracking control of port-controlled hamiltonian systems via generalized canonical transformations. *Automatica*, 39(12):2059–2069, 2003.

[17] João Erick de Mattos Fernandes, Flávio Luiz Cardoso-Ribeiro, and Mauricio Andrés Varela Morales. A port-hamiltonian model of airplane longitudinal dynamics. *IFAC-PapersOnLine*, 58(6):125–130, 2024. 8th IFAC Workshop on Lagrangian and Hamiltonian Methods for Nonlinear Control LHMNC 2024.

[18] Bernard M Maschke and Arjan J van der Schaft. Port-controlled Hamiltonian systems: modelling origins and forms. In *Proceedings of the 2nd IFAC Symposium on Nonlinear Control Systems (NOLCOS)*, pages 707–712, 1992.

[19] Brian L. Stevens and Frank L. Lewis. *Aircraft Control and Simulation*. John Wiley and Sons, 2016.

[20] Antonius A. Lambregts. Vertical flight path and speed control autopilot design using total energy principles. *AIAA*, 1983.